Drift–Alfven Instabilities and Turbulence of Magnetic Field Aligned Shear Flows

Mikhailenko V. V.[1], Mikhailenko V. S.[2] and Lee H. J.[3]

[1]BK21 Plus Information Technology, Pusan National University, Busan 609–735, South Korea
[2]Plasma Research Center, Pusan National University, Busan 609–735, South Korea
[3]Department of Electrical Engineering, Pusan National University, Busan 609–735, South Korea

Corresponding Author: vsmikhailenko@pusan.ac.kr

Abstract:

In the parallel shear flow of plasmas with inhomogeneous ion temperature comparable with or above the electron temperature two distinct drift–Alfven instabilities may be developed: the electron kinetic drift–Alfven instability, which develops due to the coupled action of the electron Landau damping and parallel velocity shear, and the ion kinetic drift–Alfven instability, which develops due to the coupled reinforcing action of parallel flow shear, ion temperature gradient and ion Landau damping. The results of the numerical investigations of these instabilities and corresponding turbulence of the parallel shear flow with inhomogeneous ion temperature are given.

1 Introduction

The magnetic field aligned plasma shear flows, which are observed in the edge layers of tokamak plasmas[1, 2, 3, 4] are the additional sources of free energy for the electrostatic and electromagnetic instabilities development. The majority of analysis of these instabilities have been restricted to the case of cold ions with ion temperature T_i much less than the electron temperature T_e. For the tokamak plasma, the ionosphere and the solar wind plasmas the case of warm ions having the temperature comparable with or even exceeding the electron temperature is more relevant.

In parallel shear flows with hot ions, $T_i \gtrsim T_e$, the ion kinetic effects play the decisive role in the development the instabilities of the parallel shear flows. In particular, such plasma is prone to the excitation of the shear-flow driven instabilities [5, 6]. It was obtained [6], that in plasma with inhomogeneous density the ion kinetic drift–Alfven instability develops from the coupled action of the parallel–flow shear and ion Landau damping. The growth rate of this instability is of the order of the frequency, the phase velocity of perturbations along the magnetic field is comparable with ion thermal veloc-

ity. The electromagnetic response of the ions for this instability is comparable with the electromagnetic response of the electrons.

In this report, we present the results of the investigations of the drift–Alfven instabilities and corresponding turbulence of the shear flow with inhomogeneous ion temperature, which develops due to the coupled reinforcing action of parallel flow shear, ion temperature gradient and the electron/ion Landau damping.

2 The drift–Alfven instabilities of parallel shear flow with inhomogeneous ion temperature

The tokamak plasma is, as a rule, a low β plasma, with $1 \gg \beta \gg m_e/m_i$. It is well known, that such plasma is unstable against the development of the electromagnetic drift–Alfven instabilities[7]. These instabilities are governed by the Vlasov equations for the electrons and ions and Poisson equation and Ampere's law for the electrostatic potential Φ and along magnetic field component A_z of the electromagnetic potential. For low frequency electromagnetic modes with frequency ω much less then the ion cyclotron frequency ω_{ci} of the inhomogeneous, magnetic- field-aligned, single–ion–species, collisionless plasma flow with velocity $\mathbf{V}_0(X_\alpha) \parallel B_0\mathbf{e}_z$ the general dispersion equation that accounts for the parallel–flow shear and inhomogeneous profiles of plasma density and of the ion temperature and accounts for the effects of thermal motion of ions, both along and across the magnetic field, has a form

$$A + i\sqrt{\pi}W\left(z_i\right)B = 0, \tag{1}$$

where

$$\begin{aligned} A = \left(1 + iz_e\sqrt{\pi}W\left(z_e\right)\right)\left(\tau z_i + \chi_i\right)\Big[\left(z_i - \chi_i\right)\left(2A_{0i} - 1\right) - z_i A_{0i}\left(S_i + \eta_i\chi_i z_i\right) \\ +2\eta_i\chi_i\, k_\perp^2\rho_i^2\left(A_{0i} - A_{1i}\right)\Big] + \Big[1 + \tau\left(1 + i\left(z_e - \chi_e\right)\sqrt{\pi}W\left(z_e\right)\right) - A_{0i}\left(S_i + \eta_i\chi_i z_i\right)\Big] \\ \times\left(\frac{k^2\rho_i^2}{2\beta} + \frac{S_i A_{0i}}{2} - A_{0i}z_i\left(z_i Q_i - \chi_i\right) + \eta_i\chi_i z_i\Big[A_{0i}z_i^2 - k_\perp^2\rho_i^2\left(A_{0i} - A_{1i}\right)\Big]\right) \\ +\Big[A_{0i}\left(z_i Q_i - \chi_i\right) - \eta_i\chi_i z_i\Big[A_{0i}z_i^2 - k_\perp^2\rho_i^2\left(A_{0i} - A_{1i}\right)\Big]\Big]^2 \end{aligned} \tag{2}$$

and

$$\begin{aligned} B = \left(A_{0i}\left(z_i Q_i - \chi_i\right) + \eta_i\chi_i\left[A_{0i}\left(\frac{1}{2} - z_i^2\right) + k_\perp^2\rho_i^2\left(A_{0i} - A_{1i}\right)\right]\right) \\ \times\left[\frac{k^2\rho_i^2}{2\beta} + \frac{S_i A_{0i}}{2} - z_i\left(z_i - \chi_i\right)\left(1 - A_{0i}\right) + \eta_i\chi_i z_i\, k_\perp^2\rho_i^2\left(A_{0i} - A_{1i}\right)\right] = 0. \end{aligned} \tag{3}$$

In Eqs.(2), (3) ω_{ci} and $\rho_i = v_{Ti}/\omega_{ci}$ is the ion thermal Larmor radius, $\tau = T_i/T_e$, $A_{ni} = I_n\left(k_\perp^2\rho_i^2\right)e^{-k_\perp^2\rho_{i,e}^2}$, I_n is the modified Bessel function of order n, $z_{i,e} = \omega/\sqrt{2}k_z v_{Ti,e}$, $W\left(z\right)$ is the complex error function, $S_i = k_y V_0'/k_z\omega_{ci}$, $Q_i = 1 - S_i$, $v_{di,e} = \left(cT_{i,e}/eB_0\right)\left(d\ln n_i/dx\right)$

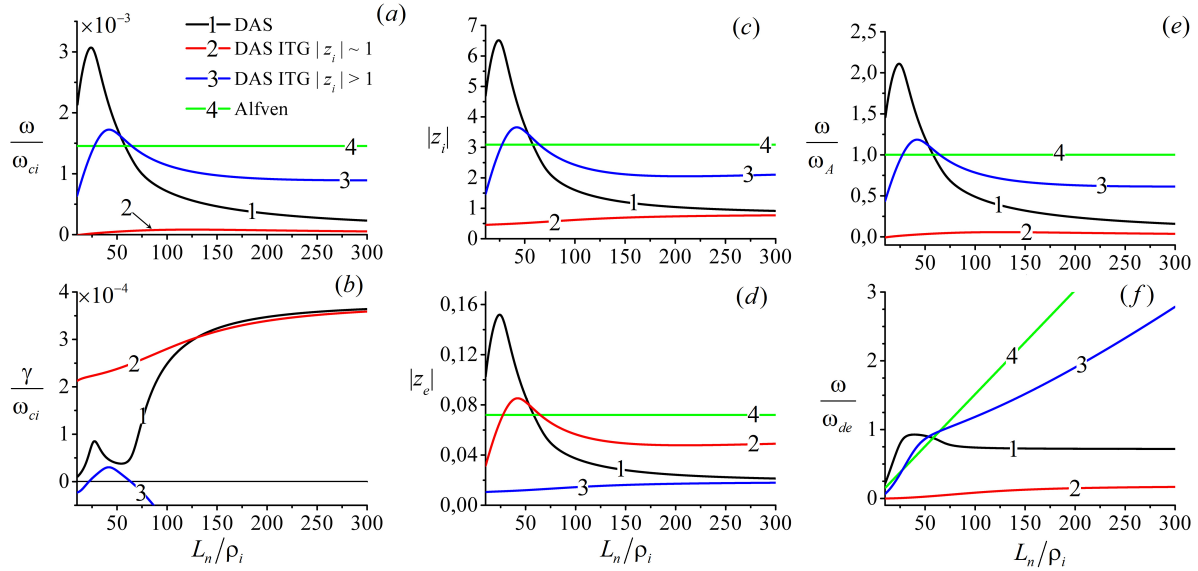

FIG. 1: The normalized frequency ω/ω_{ci} (a), the normalized growth rate γ/ω_{ci} (b), $|z_i|$ (c) and $|z_e|$ (d) versus L_n/ρ_i for $\eta_i = 3$, $k_y\rho_i = 0.1$, $T_i/T_e = 1$, $(V_0'/\omega_{ci})^{-1} = 70$, $(k_z\rho_i)^{-1} = 3000$ and $\beta = 5\%$.

is ion, electron diamagnetic velocity, $\eta_i = d\ln T_i/d\ln n_i$, $\chi_{i,e} = k_y v_{di,e}/\sqrt{2}k_z v_{Ti,e}$. The principal difference of the Eq.(1) from a similar equation obtained earlier consists in the accounting for the perturbed ion current, as well as the electron current. We do not assume here, that the phase velocity of the perturbations is much above the ion thermal velocity. In the case $T_i \sim T_e$ and $|z_{0i}| \sim 1$ the electron and ion responses in Eq.(1) are of the same order.

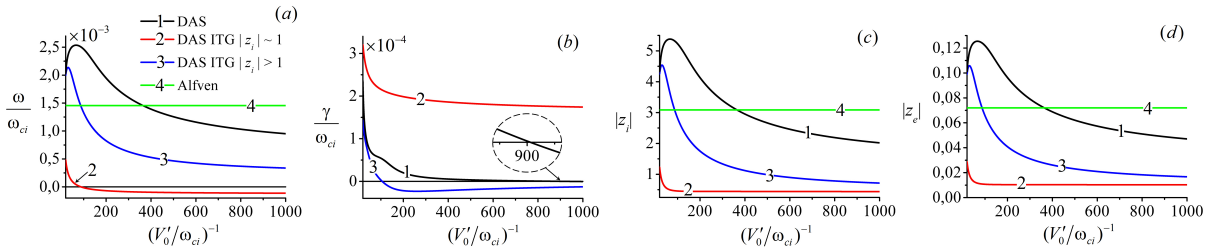

FIG. 2: The normalized frequency ω/ω_{ci} (a), the normalized growth rate γ/ω_{ci} (b), $|z_i|$ (c) and $|z_e|$ (d) versus $(V_0'/\omega_{ci})^{-1}$ for $L_n/\rho_i = 35$, $\eta_i = 3$, $k_y\rho_i = 0.1$, $T_i/T_e = 1$, $(k_z\rho_i)^{-1} = 3000$ and $\beta = 5\%$.

In the case of the homogeneous ion temperature, i.e. for $\eta_i = 0$, Eq. (1) is identical to dispersion equation obtained earlier in Ref. [6]. It was found in Ref.[6], that in a parallel plasma shear flow with inhomogeneous density but homogeneous ion temperature two distinct drift–Alfven instabilities develop. In this report, the numerical analysis of Eq.(1) is performed with particular intent to ascertain the role the ion temperature inhomogeneity on the drift–Alfven instabilities in the presence of parallel-velocity shear.

In a general case all terms in Eq.(1) are of the same order of value and the numerical analysis of Eq.(1) is necessary. In Fig.1, we present the results of the numerical solution of the dispersion equation (1) for the normalized frequency ω/ω_{ci} (a), the normalized growth rate γ/ω_{ci} (b), $|z_i|$ (c) and $|z_e|$ (d) versus L_n/ρ_i for $\eta_i = 3$, $k_y\rho_i = 0.1$, $T_i/T_e = 1$, $(V_0'/\omega_{ci})^{-1} = 70$, $(k_z\rho_i)^{-1} = 3000$ and $\beta = 5\%$. In that figure, as well as in all others, the plots for the kinetic Alfven wave in a steady plasma are denoted by a green line (4), for the drift–Alfven wave in the shear flow (DAS) with homogeneous ion temperature are denoted by a black line (1). We found, that solution to Eq.(1) predicts the development of two distinct drift–Alfven instabilities in parallel shear flow with inhomogeneous ion temperature (DAS–ITG instabilities), which may develop simultaneously under the same plasma parameters. It is a peculiarity of the drift–Alfven instabilities of the parallel shear flow with inhomogeneous ion temperature. The plots for the frequency and the growth rate of the first DAS–ITG instability are denoted by a red line (2). The plots for the second DAS–ITG instability are denoted by a blue line (3). It follows from panels (a), (b) that the growth rate $\gamma(\mathbf{k})$ of the first instability is much larger than the frequency $\omega(\mathbf{k})$. Fig.1 (c) reveals that $|z_i| \lesssim 1$ for this instability, i.e. it is developed under strong ion Landau damping and the useful estimate for the growth rate

$$\gamma \sim k_z v_{Ti}. \tag{4}$$

follows. This instability may be named as the DAS–ITG ion kinetic instability.

The growth rate of the second DAS–ITG instability (panel (b)) is much less than the frequency (panel (a)). This instability exists in the finite domain of the parameter L_n/ρ_i where plasma density inhomogeneity is sufficiently strong, and in the region of the maximum values of z_e, i.e. where the electron Landau damping is strongest and the ion Landau damping is exponentially small with $|z_i| \gg 1$. Therefore that instability is the electron kinetic. Fig. 1 (panels (e) and (b)) displays that the electron kinetic DAS–ITG instability develops in the parameters region, where its frequency is above the frequency of the kinetic Alfven wave. The same property was observed for the shear flow modified electron kinetic drift–Alfven instability of the plasma flow with homogeneous ion temperature[6]. As it follows from panel (f) of Fig.1, the frequency of the electron kinetic DAS–ITG instability in the parameters regions where the growth rate is maximum may be estimated as

$$\omega \sim k_y v_{di}. \tag{5}$$

In Fig.2, the solution of equation (1) is given for the normalized frequency ω/ω_{ci} (a), the normalized growth rate γ/ω_{ci} (b), $|z_i|$ (c) and $|z_e|$ (d) versus $(V_0'/\omega_{ci})^{-1}$ for $L_n/\rho_i = 35$, $\eta_i = 3$, $k_y\rho_i = 0.1$, $T_i/T_e = 1$, $(k_z\rho_i)^{-1} = 3000$ and $\beta = 5\%$. Fig. 2 displays, that the growth rates of both DAS–ITG instabilities have maximum values for the maximum of the velocity shearing rate. The ion kinetic DAS–ITG instability continues to exist at the reduced velocity shear, whereas the electron kinetic DAS–ITG instability exists only at the limited range of the sufficiently large velocity shear. It follows from panel (b), that electron kinetic instability is developed, when the velocity shearing rate is above the threshold value; for the employed numerical data it occurs when $V_0' > 10^{-2}\omega_{ci}$.

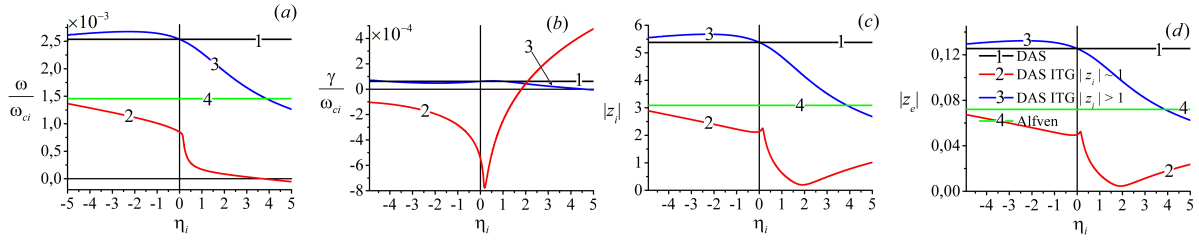

FIG. 3: The normalized frequency ω/ω_{ci} (a), the normalized growth rate γ/ω_{ci} (b), $|z_i|$ (c) and $|z_e|$ (d) versus η_i for $L_n/\rho_i = 35$, $(k_z\rho_i)^{-1} = 3000$, $k_y\rho_i = 0.1$, $(V_0'/\omega_{ci})^{-1} = 70$, $T_i/T_e = 1$ and $\beta = 5\%$.

In Fig.3, the solution of equation (1) is given for the normalized frequency ω/ω_{ci} (a), the normalized growth rate γ/ω_{ci} (b), $|z_i|$ (c), and $|z_e|$ (d) versus η_i for $L_n/\rho_i = 35$, $k_y\rho_i = 0.1$, $T_i/T_e = 1$, $(V_0'/\omega_{ci})^{-1} = 70$, $(k_z\rho_i)^{-1} = 3000$ and $\beta = 5\%$. This figure displays that the ion temperature inhomogeneity has different effect on the discovered DAS–ITG instabilities. The electron kinetic DAS–ITG instability gradually decays with growth of the parameter $\eta_i \sim L_n/L_{Ti}$. At the same time the ion temperature inhomogeneity has a decisive impact on the development of the ion kinetic DAS–ITG instability. It develops when parameter η_i becomes larger the threshold value with the growth rate growing with η_i growth. Therefore, only ion kinetic instability may be considered as the DAS–ITG instability in parallel shear flow driven by the ion temperature gradient (DAS–ITG driven instability).

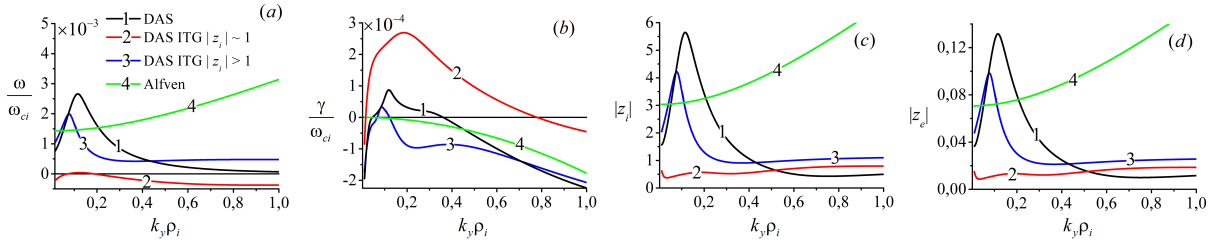

FIG. 4: The normalized frequency ω/ω_{ci} (a), normalized growth rate γ/ω_{ci} (b), $|z_i|$ (c) and $|z_e|$ (d) versus $k_y\rho_i$ for $L_n/\rho_i = 35$, $\eta_i = 3$, $(V_0'/\omega_{ci})^{-1} = 70$, $T_i/T_e = 1$, $(k_z\rho_i)^{-1} = 3000$ and $\beta = 5\%$.

In Fig. 4, the solution to Eq.(1) is given for the normalized frequency ω/ω_{ci} (a), the normalized growth rate γ/ω_{ci} (b), $|z_i|$ (c) and $|z_e|$ (d) versus $k_y\rho_i$ for $L_n/\rho_i = 35$, $\eta_i = 3$, $(V_0'/\omega_{ci})^{-1} = 70$, $T_i/T_e = 1$, $(k_z\rho_i)^{-1} = 3000$ and $\beta = 5\%$. This figure reveals, that for the employed parameters the electron kinetic DAS–ITG instability develops in the narrow interval $\sim 0.05 \div 0.15$ of the $k_y\rho_i$ values with the growth rate much less than the frequency. At the same parameters, the ion kinetic DAS–ITG instability develops with the growth rate much above the frequency in the wide interval $\sim 0.05 \div 0.8$ of the $k_y\rho_i$ values. Note, that the frequency of the ion kinetic DAS–ITG instability changes its sign in this interval: it becomes positive in the narrow region of $k_y\rho_i$ where the growth rate is maximum being

negative at the rest part of the $k_y\rho_i$ values.

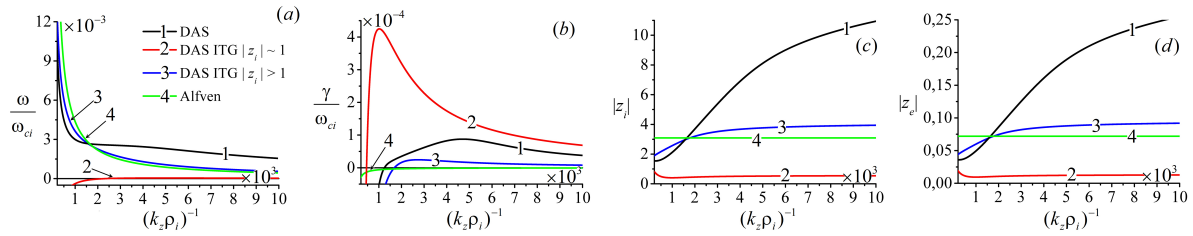

FIG. 5: The normalized frequency ω/ω_{ci} (a), the normalized growth rate γ/ω_{ci} (b), $|z_i|$ (c) and $|z_e|$ (d) versus $(k_z\rho_i)^{-1}$ for $L_n/\rho_i = 35$, $\eta_i = 3$, $k_y\rho_i = 0.1$, $(V_0'/\omega_{ci})^{-1} = 70$, $T_i/T_e = 1$ and $\beta = 5\%$.

In Fig.5, the solution to equation (1) is given for the normalized frequency ω/ω_{ci} (a), the normalized growth rate γ/ω_{ci} (b), $|z_i|$ (c) and $|z_e|$ (d) versus $(k_z\rho_i)^{-1}$ for $L_n/\rho_i = 35$, $\eta_i = 3$, $k_y\rho_i = 0.1$, $(V_0'/\omega_{ci})^{-1} = 70$, $T_i/T_e = 1$ and $\beta = 5\%$. The panel (b) displays that the ion kinetic DAS–ITG instability has largest growth rate in comparison with electron kinetic DAS–ITG instability and DAS instability of a plasma with homogeneous ion temperature for all considered value of $(k_z\rho_i)^{-1}$. More over, the maximum growth rate of the ion kinetic DAS–ITG instability attains for $(k_z\rho_i)^{-1}$ values ($(k_z\rho_i)^{-1} \approx 10^{-3}$) for which other considered instabilities does not developed.

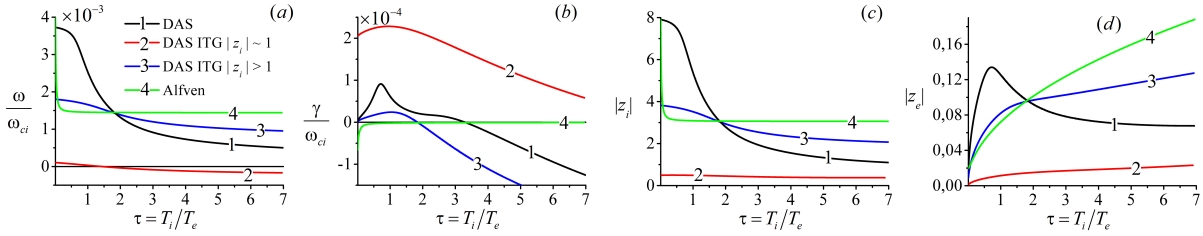

FIG. 6: The normalized frequency ω/ω_{ci} (a), the normalized growth rate γ/ω_{ci} (b), $|z_i|$ (c) and $|z_e|$ (d) versus $\tau = T_i/T_e$ for $L_n/\rho_i = 35$, $\eta_i = 3$, $k_y\rho_i = 0.1$, $(V_0'/\omega_{ci})^{-1} = 70$,$(k_z\rho_i)^{-1} = 3000$ and $\beta = 5\%$.

In Fig.6, the solution to equation (1) is given for the normalized frequency ω/ω_{ci} (a), the normalized growth rate γ/ω_{ci} (b), $|z_i|$ (c) and $|z_e|$ (d) versus $\tau = T_i/T_e$ for $L_n/\rho_i = 35$, $\eta_i = 3$, $k_y\rho_i = 0.1$, $(V_0'/\omega_{ci})^{-1} = 70$,$(k_z\rho_i)^{-1} = 3000$ and $\beta = 5\%$. This figure displays that the DAS instability, electron and ion kinetic DAS-ITG instabilities develop in parallel shear flow with warm ions. The maximum growth rate attains for the plasma with $T_i \approx T_e$ (DAS instability) or when $T_i \gtrsim T_e$ (both DAS–ITG instabilities). Panel (b) demonstrates that DAS and electron kinetic DAS–ITG instabilities exist in the finite ion/electron temperatures ratio, whereas the ion kinetic DAS–ITG instability exists on the all considered values of the temperatures ratio.

3 Transport estimates

The performed numerical analysis of the dispersion equation (1) displays the existence of the shear flow driven ion kinetic DAS–ITG instability with the growth rate much above the frequency. This growth rate is also much above the frequency of the electron kinetic DAS–ITG instability, which has the growth rate much less than the frequency. The initially fastest growing disturbance due to the ion kinetic DAS–ITG instability will dominate the subsequent development the drift–Alfven turbulence in parallel shear flow. Certainly, the nonlinear analysis of this instability can't be performed on the base of the weak turbulence approach. Also, the renormalized nonlinear theory[8], which accounts for the scattering of ions by the ensemble of waves with random phases can't be applied to this instability. The phase randomization of the waves in the wave packet with wave number spectrum width $\Delta k_\perp \sim k_\perp$ and the frequency $\omega(\mathbf{k})$ occurs at time $t \sim \gamma^{-1}(\mathbf{k})$ when

$$\frac{d\omega(\mathbf{k})}{dk_\perp}\Delta k_\perp t \sim \frac{\omega(\mathbf{k})}{\gamma(\mathbf{k})} \gtrsim \pi, \tag{6}$$

but this does not occur for the ion kinetic DAS–ITG instability. There is no small parameter which can be applied for the development of any kind of the turbulence theory. At the most general level we employ here the widely invoked "mixing length estimate" for the saturated amplitude of the electric field. It balances the wavelength of the perturbation against the particle (in our case the ion) displacement, ξ, in the unstable electric field,

$$\xi \sim \frac{u}{\gamma} \sim \frac{2\pi}{k_\perp}. \tag{7}$$

Eq. (7) defines the threshold for stochastization or mixing of a test ion trajectory and is the familiar for the instability saturation level[9]. With the estimates (4) for the growth rate $\gamma \sim k_z v_{Ti}$ and for the ion velocity $u \sim cE/B \sim ck_\perp\varphi/B$, Eq. (7) gives the estimate

$$\frac{e\varphi}{T_i} \sim \frac{k_z}{k_\perp}\frac{2\pi}{k_\perp\rho_i}. \tag{8}$$

This estimate is the same as was obtained in Ref.[10] for the perturbed potential in the steady state of the ion kinetic shear flow driven drift–Alfven (DAS) instability of a plasma with homogeneous ion temperature. DAS instability has comparable the frequency and the maximum growth rate, $\omega(\mathbf{k}) \sim \gamma(\mathbf{k}) \sim k_z v_{Ti}$. Note, that the estimate (8) was obtained in Ref.[10] employing the renormalized nonlinear theory, which accounts for the scattering of ions by the ensemble of waves with random phases.

The mixing length estimate may be employed for the determining the steady state level for the electron kinetic DAS–ITG instability. In this case balance equation has a form

$$\xi \sim \frac{u}{\omega} \sim \frac{2\pi}{k_\perp}, \tag{9}$$

where the estimate for the frequency ω is given by Eq.(5). The estimate for the steady state level for the perturbed potential,

$$\frac{e\varphi}{T_i} \lesssim \frac{1}{k_\perp L_n}, \tag{10}$$

appeared to be the same as the obtained in Ref.[10] for the electron kinetic shear flow modified drift- Alfven instability.

4 Conclusions

The comprehensive analysis of the dispersion equation (1), which accounts for the parallel flow shear, the inhomogeneous profiles of the plasma density and of the ion temperature and accounts for the effects of thermal motion of ions was performed. It was obtained, that the parallel shear flow of a plasma with inhomogeneous ion temperature of the order or above the electron temperature ($T_i \gtrsim T_e$) is unstable against the development of the specific ion kinetic DAS–ITG instability the growth rate of which much above the frequency. This instability develops in a wide interval of the wave numbers and is a source of the development of the drift-Alfven turbulence. The level of the turbulence in he steady state is determined invoking the "mixing length" estimate.

This work was supported by National R&D Program through the National Research Foundation of Korea (NRF) funded by the Ministry of Education, Science and Technology (Grant No. NRF-2014M1A7A1A03029878) and BK21PLUS.

References

[1] ASAKURA, N., et al. J. Nucl. Mater. 313, 820 (2003).

[2] LABOMBARD, B., et al., Nucl. Fusion 44, 1047 (2004).

[3] FEDORCZAK, N. et al., Journal of Nuclear Materials 390–391, 368 (2009).

[4] PEDROSA, M.A., et al., Plasma Phys. Control. Fusion 46, 221 (2004).

[5] MIKHAILENKO, V.V. et al. Phys.Plasmas 21, 072117 (2014).

[6] MIKHAILENKO, V.V. et al., Physics of Plasmas 23, 020701 (2016)

[7] MIKHAILOVSKII A.B.,Electromagnetic Instabilities in an Inhomogeneous Plasma. Institute of Physics Publishing, Bristol, 1992.

[8] DUM, C.T., DUPREE, T.H. , Phys. Fluids, **13**, 2064 (1971).

[9] DIAMOND, P.H., et al., Modern Plasma Physics. Vol.1 : Physical Kinetics of Turbulent Plasmas. Cambridge University Press, 2010, p. 144.

[10] MIKHAILENKO, V.V. et al., Physics of Plasmas 23, 092301 (2016)